Developmental Biology **249,** 283–299 (2002)
doi:10.1006/dbio.2002.0770

Novel Behavioral and Developmental Defects Associated with *Drosophila single-minded*

Jan Pielage,* Georg Steffes,* Dan C. Lau,† Beth A. Parente,† Stephen T. Crews,† Roland Strauss,‡ and Christian Klämbt*,[1]

**Institut für Neurobiologie, Universität Münster, Badestrasse 9, D-48149 Münster, Germany; †Department of Biochemistry, The University of North Carolina at Chapel Hill, Chapel Hill, North Carolina 27599-3280; and ‡Theodor-Boveri-Institut für Biowissenschaften, LS Genetik und Neurobiologie, Am Hubland, D-97074 Würzburg, Germany*

In *Drosophila,* the development of the midline cells of the embryonic ventral nerve cord depends on the function of the bHLH-PAS transcription factor Single-minded (Sim). The expression domain of *sim,* however, is also found anterior and posterior to the developing ventral cord throughout the germ band. Indeed, mutations in *sim* were identified based on their characteristic cuticle phenotype. Eight abdominal segments (A1–A8) can be easily seen in the larval cuticle, while three more can be identified during embryogenesis. Cells located in A8–A10 give rise to the formation of the genital imaginal discs, and a highly modified A11 segment gives rise to the anal pads that flank the anus. *sim* is expressed in all these segments and is required for the formation of both the anal pads and the genital imaginal discs. A new temperature-sensitive *sim* allele allowed an assessment of possible postembryonic function(s) of *sim*. Reduction of *sim* function below a 50% threshold leads to sterile flies with marked behavioral deficits. Most mutant *sim* flies were only able to walk in circles. Further analyses indicated that this phenotype is likely due to defects in the brain central complex. This brain region, which has previously been implicated in the control of walking behavior, expresses high levels of nuclear Sim protein in three clusters of neurons in each central brain hemisphere. Additional Sim localization in the medullary and laminar neurons of the optic lobes may correlate with the presence of ectopic axon bundles observed in the optic lobes of *sim* mutant flies.

***Key Words: single-minded*; *Drosophila*; CNS; midline; genital disc; brain; behavior.**

INTRODUCTION

First signs of *Drosophila* nervous system development are evident only a few hours after fertilization during the cellular blastoderm stage. At this time point, maternal gene functions have divided the embryo into the three germ layers (Campos-Ortega and Hartenstein, 1997). The mesodermal anlage is separated from the lateral neurogenic region by a very special set of cells, which have been recognized as an important part of the ventral nerve cord some 100 years ago (Escherich, 1902). Based on morphological criteria, these cells were later called mesectodermal cells (Poulson, 1950). These are the first neural cells to be specified (Crews *et al.,* 1988) and are initially arranged in a single cell-wide row with about four cells per hemisegment. Following gastrulation, when the mesoderm has invaginated into the interior of the embryo, the mesectodermal cells intermingle at the ventral midline and move into the interior of the embryo. Here, they form a mitotic domain and generate a small number of neuronal and glial cells located at the midline of the developing ventral cord (Bossing and Technau, 1994; Foe, 1989; Klämbt *et al.,* 1991; Thomas *et al.,* 1988). A number of studies have shown that the midline cells are distinct from the remaining neural cells in a number of ways (Crews, 1998; Jacobs, 2000).

The CNS midline cells exert many prominent functions during CNS development. The loss of all CNS midline cells, which are the source of attractive (Netrins) and repulsive (Slit) axonal guidance cues, leads to a dramatic axonal patterning phenotype (Brose and Tessier-Lavigne, 2000; Kidd *et al.,* 1999; Mitchell *et al.,* 1996; Rothberg *et al.,* 1988, 1990; Thomas *et al.,* 1988). In addition, the CNS midline cells regulate directed cell migration toward and

[1] To whom correspondence should be addressed. Fax: +49 251 832 4686. E-mail: klaembt@mail.uni-muenster.de.

0012-1606/02 $35.00

away from the midline (Bashaw and Goodman, 1999; Kidd *et al.*, 1999; Kinrade *et al.*, 2001; Kramer *et al.*, 2001). Besides directing the migration of growth cones and cells, inductive signals emanating from the CNS midline regulate the development of cortical neurons and certain mesodermal cells (Chang *et al.*, 2000; Lüer *et al.*, 1997; Menne *et al.*, 1997; Zhou *et al.*, 1997). These findings underpin the role of the CNS midline as an important organizing center during normal embryonic development.

The special appearance and the strategic position of CNS midline cells are reflected by the fact that their cell fate is determined very early by the action of neurogenic genes (Menne and Klämbt, 1994; Morel and Schweisguth, 2000). The activation of *Notch* results in the expression of the gene *sim*, which subsequently serves as a master regulatory gene of CNS midline development (Crews *et al.*, 1988; Muralidhar *et al.*, 1993; Nambu *et al.*, 1990, 1991; Thomas *et al.*, 1988). Loss of *sim* function results in a loss of all CNS midline cells, whereas ectopic expression of *sim* within the nervous system is able to induce the midline differentiation program (Nambu *et al.*, 1991; Sonnenfeld and Jacobs, 1994). Depending on the segmental position, *sim* is able to specify glial as well as neuronal midline cell types (Menne *et al.*, 1997).

Two promoters direct the expression of two alternative *sim* transcripts. *sim* expression starts at the onset of gastrulation in the mesectodermal cells flanking the presumptive mesoderm. Initially, *sim* is expressed by all midline cells; however, during midembryogenesis, expression becomes restricted to the midline glia. In addition, a complex pattern of *sim* expression has been described in the embryonic brain (Therianos *et al.*, 1995). Outside the nervous system, *sim* expression has been reported in a subset of ventral muscle precursor cells (Lewis and Crews, 1994). *sim* expression extends beyond the developing ventral nerve cord to the abdominal-most segmental units. The function of these *sim*-expressing cells is unknown.

sim encodes a basic-helix–loop–helix–PAS (bHLH-PAS) protein that, when binding to an appropriate interaction partner, directly activates transcription. Sim can also repress gene expression in the midline cells by activating the transcription of repressive factors (Estes *et al.*, 2001). To date, two direct interaction partners have been described: Dichaete (Fish-hook), which associates with the PAS domain of Sim, and the bHLH-PAS protein encoded by *tango* (*tgo*) (Ma *et al.*, 2000; Ohshiro and Saigo, 1997; Sonnenfeld *et al.*, 1997; Soriano and Russell, 1998). Mutant *tgo* embryos display only relatively mild defects during embryonic CNS development (Ohshiro and Saigo, 1997; Sonnenfeld *et al.*, 1997). Unlike *sim*, however, *tgo* is deposited maternally in the egg, and this strong maternal contribution is likely to compensate the early requirement of *tgo*. No germline clones have yet been described. Clonal analyses demonstrate that *tgo* is required for adult antennal and tarsal development. Here, it does not interact with Sim but with the bHLH-PAS protein Spineless (Emmons *et al.*, 1999). To date, no function of *sim* has been described during postembryonic development.

Here, we report the identification of a temperature-sensitive *sim* mutation. Our data show that *sim* expression within the developing brain is important to correctly specify the formation of the central complex, a part of the brain required to control the walking behavior of the fly. In addition, we show that *sim* is required outside the CNS to correctly pattern the genital discs as well as the anal pad anlage.

MATERIALS AND METHODS

Genetics

Among the mutations identified in a large-scale EMS mutagenesis (Hummel *et al.*, 1999), we identified the sim^{ts} mutation. The mutation was subsequently separated from other lethal hits found on this particular chromosome by recombination against *rucuca* chromosomes. The amorphic sim^{H9} allele and the enhancer trap line $P[lacW]esc^{B7\text{-}2\text{-}22}$ were obtained from the Bloomington Stock Center.

Behavioral Analyses

Walking was quantified in Buridan's paradigm (Götz, 1980). Wings were clipped under cold anesthesia (4°C) in order to ensure that flies will only walk. Flies were then given at least 4 h to recover in single-fly containers with access to water before they were placed on an elevated circular disc (diameter 85 mm) between two opposing and inaccessible landmarks in an otherwise uniform bright white surrounding (3000 cd m^{-2}). The dark vertical landmarks were 100 mm away from the center of the disc and appeared under viewing angles of 11° horizontally and 58° vertically. The disc was surrounded by a water-filled moat. The walking-trace of each fly was recorded for 15 min by using a video-based computerized tracking system (time resolution 5 frames s^{-1}). The traces were evaluated off-line with regard to walking speed, activity, walked distance, and orientation toward the landmarks as described (Strauss and Pichler, 1998). *Walking speed* is calculated for every transition of the fly from one landmark to the other. Start and end of a transition are defined by the crossing of parallel lines which are perpendicular to the connecting axis of the two landmarks and which intersect with it at +33 mm and −33 mm as seen from the center of the disk. The mean speed of all transitions within 15 min is called the walking speed of the individual fly. *Walking activity* is defined as the fraction of time spent walking instead of resting or grooming. *Walked distance* is the total length of the piecewise linear interpolation of the fly's track given by successive positions sampled every 0.2 s. *Orientation*: For each path increment, also the angular deviation from the direct path toward each of the two landmarks is calculated. The smaller of the two angular values is always integrated into a frequency histogram. At the given sampling rate, each fly contributes 4500 orientation values in a 15-min measurement, that were integrated in a frequency histogram of 5° bin width. For a direct comparison, the same four evaluations were also applied to random search measurements, where the flies saw no landmarks.

Leg coordination of *sim* flies was inspected on a walking analyzer as described (Strauss, 1998). Briefly, the fly walks on a glass plate which is overlaid with a layer of red laser light invisible to the

fly. The light carpet is so thin that only legs are illuminated which are either in contact to the ground or near touch-down. The points of ground contact are registered by cameras underneath the glass plate and the temporal and spatial aspects of stepping are analyzed off-line on a PC.

Molecular Analyses

Total RNA was extracted from different stages of $y\ w^{67}$ by using QIAshredder and RNeasy kits (Qiagen). RNA was treated with RNase-free DNase I (RQ1; Promega) to remove contaminating genomic DNA. Stages and dissected tissues were: (1) 0–18 h (AEL) embryos, (2) wandering third instar larvae, (3) wandering third instar larval brains, (4) pupae, and (5) adults (male and female combined). Synthesis of cDNA was performed by using SuperScript reverse transcriptase and the primer, 5′-CTGGTTGATGTGCG-GATG-3′, which corresponds to the 3′ end of *sim* exon 4. PCR was carried out by using the primer pair, 5′-GCCTGGGGCTCATC-GCCT-3′ (5′ end of exon 3) and 5′-CAGCGACAAAATGGC-ATTC-3′ (region of exon 4 just 5′ to the primer used for cDNA synthesis). The primer pair was derived from two exons, so that amplification of contaminating genomic DNA could be distinguished from the amplified products derived from RT-PCR of RNA. Two controls were included. Genomic DNA was PCR amplified by using the primers described above to yield a 558-bp fragment. Presence of this band in RT-PCR-amplified *Drosophila* RNA samples would indicate the presence of contaminating genomic DNA. Positive control sample involved RT-PCR amplification of RNA synthesized from a full-length *sim* cDNA clone transcribed *in vitro* with SP6 RNA Polymerase. This yielded a DNA fragment of 237 bp and corresponds to the RT-PCR-amplified products derived from *Drosophila* RNA. PCR products were subjected to agarose gel electrophoresis, stained with ethidium bromide, and visualized for fluorescence.

Sequence Analysis of sim^{J1-47} Mutant sim Gene

The complete coding sequence of the *sim* gene from sim^{J1-47} homozygous mutant adult flies was determined by using PCR amplification of isolated genomic DNA sequence followed by direct sequencing of the PCR products. Multiple primer pairs (details provided upon request) and *Taq* polymerase were used to PCR amplify DNA containing exons 2–8, which contain all of the *sim* coding sequence. Fragments were gel purified and sequenced by using an ABI automated sequencer. Each fragment was independently amplified multiple times, and both strands were sequenced.

Immunohistochemistry

Embryos were collected and stained as described previously (Hummel *et al.*, 1997). Wandering third instar larvae were dissected in PBT and fixed in 4% formaldehyde on ice for 1 h. Antibody staining was performed as described (Patel *et al.*, 1987). Antibody dilutions were used as follows: rat anti-Sim, 1:100; mAb anti-Tgo, 1:1; mAb anti-Eve, 1:5; mAb BP102, 1:50; mAb anti-ELAV (9F8A9; from Developmental Studies Hybridoma Bank), 1:100; and rabbit anti-β-galactosidase (Cappel), 1:2000. Larval brains were dissected in PBS after antibody staining, mounted in Aqua-Poly/Mount (Polysciences, Inc.), and visualized on a Zeiss LSM510 confocal microscope. Images were processed by using the Zeiss LSM Browser and Adobe Photoshop.

Histology

Serial 7-μm-thick paraffin sections of adult heads were prepared in frontal orientation by using the collar method (Ashburner, 1989; Heisenberg and Böhl, 1979). The brains were inspected under a fluorescence microscope.

RESULTS

Identification of a Temperature-Sensitive sim Allele

Mutations in the gene *sim* result in the loss of all CNS midline cells. Subsequently, all CNS axon tracts collapse at the CNS midline (Crews *et al.*, 1988; Klämbt *et al.*, 1991; Sonnenfeld and Jacobs, 1994; Thomas *et al.*, 1988; Figs. 1A and 1B). All *sim* mutations isolated to date lead to this typical CNS phenotype (for review, see Jacobs, 2000). We fortuitously identified a weak *sim* allele in the mutant collection established recently in the lab (Hummel *et al.*, 1999). The sim^{J1-47} mutation was subsequently isolated by standard recombination techniques. In order to avoid background effects, we generally analyzed *ru h th st cu* sim^{J1-47} e/*st* sim^{J1-47} *e ca* transheterozygous embryos (hereafter referred to as homozygous sim^{J1-47} embryos). To test whether the weak CNS phenotype associated with sim^{J1-47} results from a temperature-sensitive mutation, we analyzed the embryonic CNS phenotypes of homozygous sim^{J1-47} and sim^{J1-47}/sim^{H9} embryos at 17 and 29°C (Fig. 1).

At the permissive temperature (17°C), the CNS of homozygous sim^{J1-47} embryos appeared indistinguishable from wild type embryos (compare Figs. 1A and 1C). Furthermore, homozygous sim^{J1-47} flies eclosed (see below). However, *sim* function was not completely restored at 17°C since, in trans to the null allele sim^{H9}, a moderate CNS phenotype was detected (Fig. 1D) that is never seen in $sim^{H9}/+$ embryos. At the restrictive temperature (29°C), homozygous sim^{J1-47} embryos developed a strong midline defect. Commissures appeared fused and the connectives were found closer to the midline (Fig. 1E). The embryonic axon pattern phenotype became more severe in sim^{J1-47}/sim^{H9} embryos raised at 29°C and resembled the amorphic *sim* phenotype (compare Figs. 1B and 1F). Thus, we conclude that the allele *J1–47* represents a temperature-sensitive *sim* mutation.

The sim^{J1-47} Mutant Has a Mutation in the Sim Dimerization Domain

The *sim* gene from sim^{J1-47} homozygous mutant flies was sequenced and compared with the wild-type *sim* gene (Fig. 2). There was a single amino acid change that occurred at residue 41, resulting in a Ser > Phe substitution. The Sim protein contains a bHLH domain, in which the basic region is required for DNA binding and the HLH domain is required for dimerization to the Tgo bHLH-PAS protein. Ser41 lies within helix 2 of the HLH domain. This residue is conserved among all Sim proteins, including two *Drosophila* species and a variety of vertebrate species (Fig. 2). It

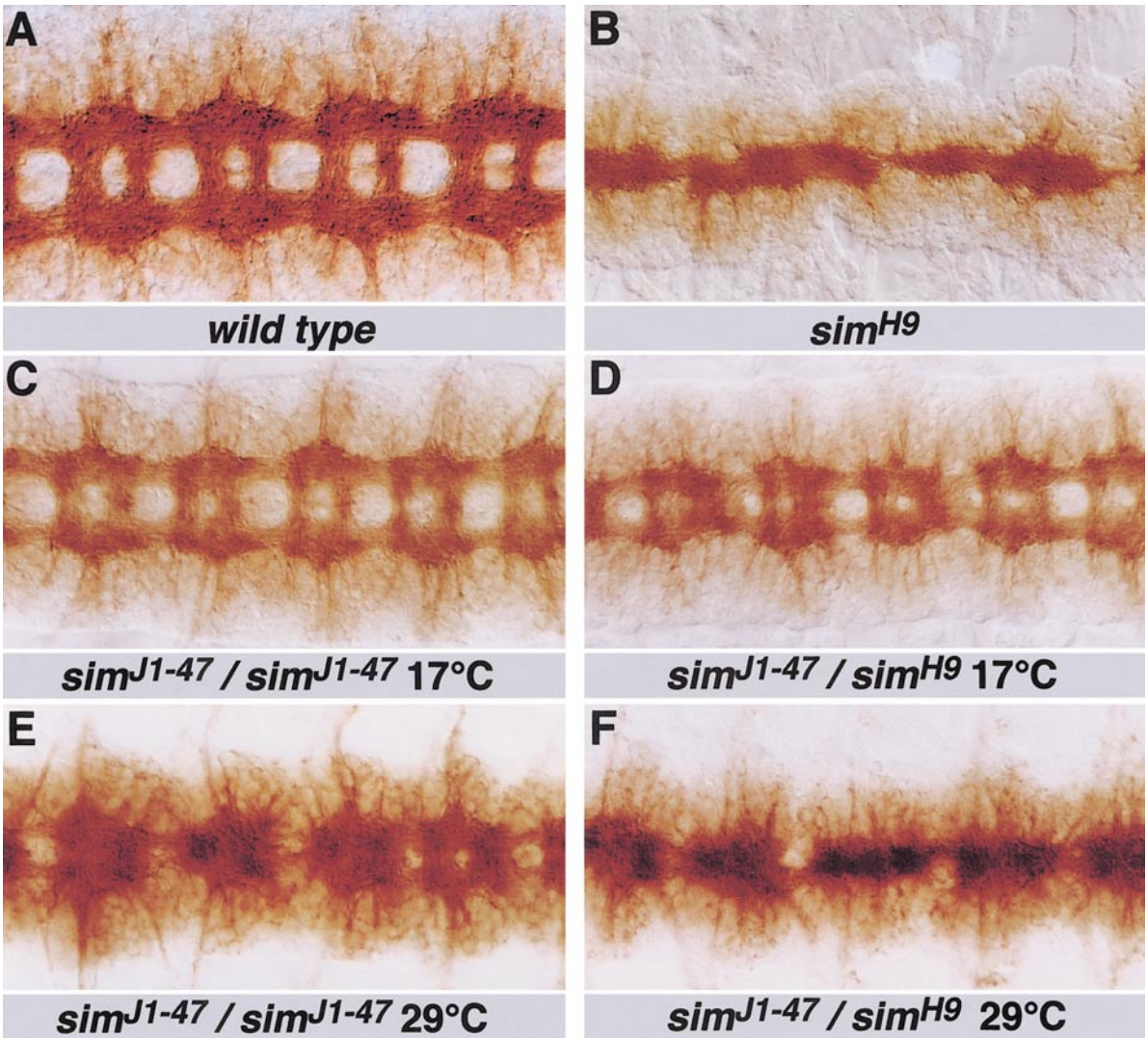

FIG. 1. Identification of a temperature-sensitive *sim* allele. Frontal views of dissected stage 16 ventral nerve cords of the indicated genotype stained for the overall axon pattern using the mAb BP102. The breeding temperature is indicated. Anterior is to the left. (A) In wild type embryos, a ladder-like axon pattern can be recognized. Axons running in the longitudinal connectives connect the different neuromeres along the a/p axis. In every neuromere, two commissures are found: the anterior commissure and the posterior commissure. (B) In sim^{H9} null mutants, all CNS axons collapse at the midline. (C) The ventral nerve cord of homozygous sim^{J1-47} embryos appears wild type and no abnormalities can be detected. (D) In sim^{J1-47}/sim^{H9} embryos grown at low temperature, a mild fused commissure phenotype develops, which is indicative of midline glial cell defects. (E) When homozygous sim^{J1-47} embryos are raised at the restrictive temperature, a strong fused commissure phenotype develops. Note that the connectives are also affected. (F) Mutant sim^{J1-47}/sim^{H9} embryos grown at the restrictive temperature show a complete collapse of the nervous system similar to the phenotype caused by the complete loss of *sim* function (B).

is also commonly conserved between related invertebrate and vertebrate bHLH-PAS proteins, including Trachealess, Hypoxia-inducible factors, and the Aryl hydrocarbon receptor. The high degree of conservation in a known functional domain strongly suggests that the Ser > Phe substitution at residue 41 is responsible for the mutant phenotype. The position of Ser41 in the protein suggests a role in influencing protein dimerization, DNA binding, or both (Ferre-D'Amare *et al.*, 1993).

Requirement of single-minded during the Development of the Larval Cuticle

Mutations in the *sim* gene were also identified based on their larval cuticle phenotype, which is characterized by defective formation of the ventral-most denticles and abnormal anal pad formation (Mayer and Nüsslein-Volhard, 1988).

In the larval cuticle, eight abdominal segments can be easily seen. In the phylotypic stage, the primordia of the

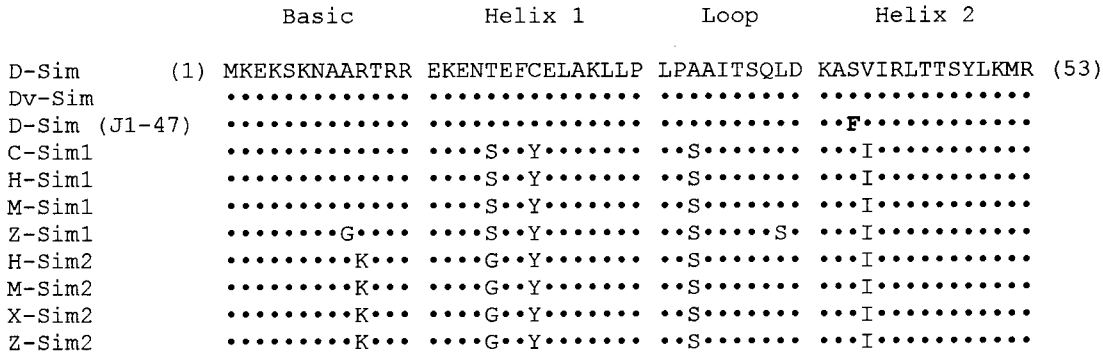

FIG. 2. Alignment of Sim proteins reveals that sim^{J1-47} has a mutation in a conserved residue in helix 2. Sequence of the entire sim^{J1-47} *sim* gene revealed only a single amino acid replacement compared with the wild type *sim* sequence: Ser41 was changed to a Phe in sim^{J1-47}. Alignment of all of the known Sim proteins, both insect and vertebrate, indicate that all contain a Ser at residue 41. Humans, mice, and other vertebrates contain at least two *Sim* genes: *Sim1* and *Sim2*. D, *Drosophila melanogaster*; Dv, *Drosophila virilis*; C, chicken; H, humans; M, murine; X, *Xenopus*; Z, zebrafish.

abdominal segments A9 and A10 can be identified. Cells located in A8–A10 contribute to the development of the genital imaginal discs. A highly modified A11 segment gives rise to the anal pads that flank the anus (Jürgens and Hartenstein, 1993). In *sim* null mutants, the anal pads formed; however, their size appeared reduced compared with wild type, and the anal slit is not developed (Fig. 3B). In homozygous sim^{J1-47} embryos grown at the permissive temperature, the anus always formed normally (Fig. 3C). In trans to the amorphic mutation sim^{H9}, the anal slit occupied only half of the anal pad (Fig. 3D, arrow). When raised at the restrictive temperature, homozygous sim^{J1-47} larvae as well as sim^{J1-47}/sim^{H9} larvae completely lacked the anal slit (Figs. 3E and 3F, arrow).

How is the defect in anal pad development mediated? During development, *sim* expression in the midline extends to the posterior end of the germ band, where it demarcates the anterior boundary of the proctodeum (Figs. 4A–4F). As the proctodeum lies within the anal pad, we analyzed possible coexpression with the anal pad marker Even skipped (Eve) (Gorfinkiel *et al.*, 1999). In stage 11 embryos, a crescent of Eve expression was seen abutting the domain of *sim* expression at the midline (Figs. 4D–4F). Confocal analyses demonstrated that Sim and Eve are never coexpressed. In *sim* null mutant embryos, the onset of Eve expression in the anal pad anlage was normal; however, Eve expression extends across the ventral midline (Fig. 4G). By the end of embryogenesis, the anal pad is reduced in size in *sim* mutants compared with wild type (Figs. 4H and 4I). Thus, both the anal pad phenotype of *sim* mutant larvae and the expression pattern described above suggest that *sim*-expressing cells contribute to the formation of the anal pads.

sim Is Required for the Development of the Genital Discs

In the abdominal segments A9 and A10, just anterior to the forming anal pads and thus within the expression domain of *sim*, lies the unpaired genital disc primordium (Hartenstein and Jan, 1992; reviewed in Jürgens and Hartenstein, 1993). To investigate whether *sim* also affects the formation of these ectodermal derivatives, we used an enhancer trap insertion in the *escargot* (*esg*) gene, which labels all imaginal discs anlagen by the end of embryogenesis (Hayashi *et al.*, 1993). In wild type embryos, a field of *esg*-expressing cells was seen posterior to the forming nervous system (not shown). Following germ band retraction, these cells invaginate into the interior of the embryo. Epidermal cells close the gap left by the delaminated disc progenitor cells, and in stage 16 embryos, a narrow strip of *esg*-positive cells was seen (Figs. 5 A, 5C, and 5E, arrows). In *sim* mutant embryos, specification of the genital disc anlage is normal as judged by the onset of *esg* expression. The invagination of the anlage starts normally as well but cannot proceed to its final state. Instead, the presumptive disc cells were found in a large ectodermal fold at the posterior end of the embryo (Figs. 5B, 5D, and 5F, arrows). Interestingly, this phenotype correlates with a defect observed in the condensation of the ventral nerve cord. *sim* expression overlaps with *esg* expression, which initially is expressed in the CNS midline as well (data not shown). At present, we cannot tell whether the genital disc phenotype is due to disruption of nerve cord condensation or whether it is due to a loss of midline cells in the disc anlage.

Adult Phenotypes Associated with sim

At the permissive temperature, homozygous sim^{J1-47} flies survived to adulthood; however, both females and males were sterile. A similar phenotype was observed in $Df(3R)ry^{614}/sim^{H9}$ or $Df(3R)ry^{75}/sim^{H9}$ flies (see Fig. 7). In the majority of the flies (>90%), no abnormal external phenotypes were detected. The remaining flies showed dramatic external phenotypes lacking genitalia as well as the anus (Figs. 6B and 6D). Instead of forming the anal plate and the external genital organs (vulva, clasper, and penis apparatus),

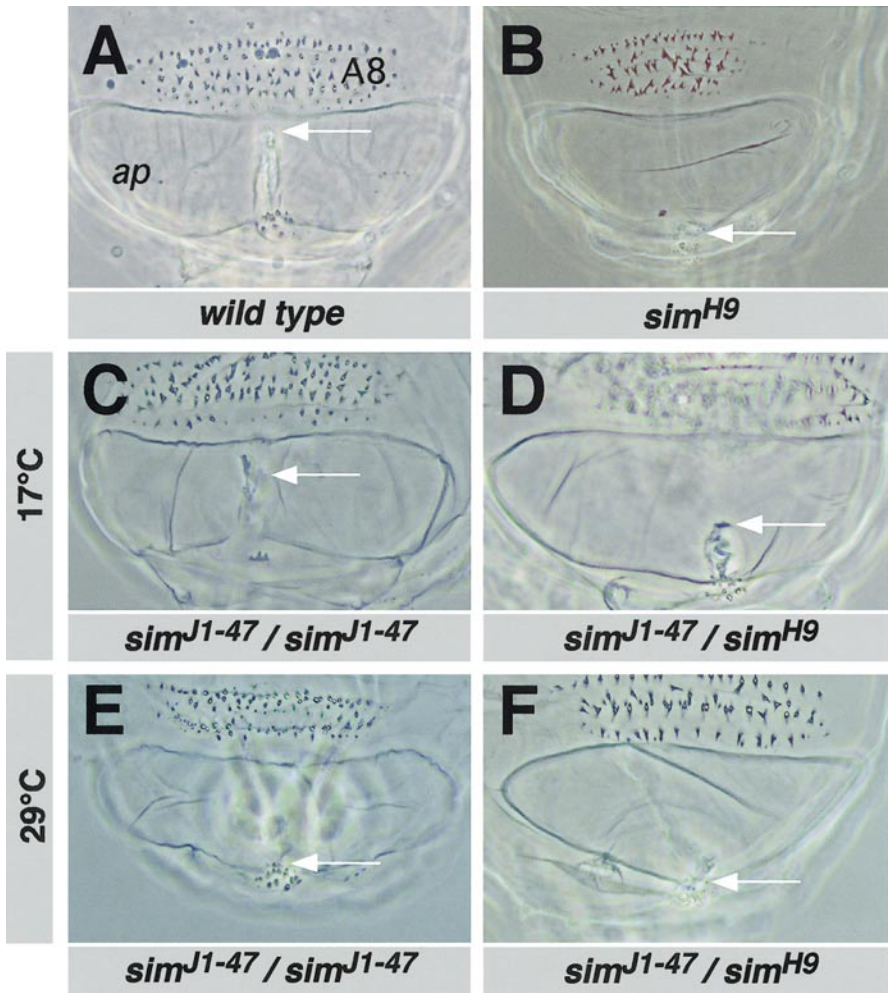

FIG. 3. Larval phenotypes associated with *sim*. Cuticle preparations of wild type and mutant *sim* larvae. Only the tail region is shown. Anterior is up. (A) Wild-type, the arrow points to the anterior origin of the anal slit in the anal pad (ap). The A8 segment is indicated. (B) Homozygous mutant sim^{H9} larvae lacking all *sim* function. The anal pad is smaller compared with wild type and no anal slit can be detected (arrow). (C) Homozygous mutant sim^{J1-47} larvae grown at the permissive temperature. The sizes of the anal pad and the anal slit are normal. (D) In sim^{J1-47}/sim^{H9} larvae grown at the permissive temperature, the anal slit is shortened (arrow). (E) Homozygous mutant sim^{J1-47} larvae grown at the restrictive temperature. The size of the anal slit is greatly reduced. (F) In sim^{J1-47}/sim^{H9} larvae grown at the restrictive temperature, the anal slit is absent.

the tergit and sternit derived from the A8 segment close the flies posteriorly (Figs. 6B′ and 6D′). We also analyzed the internal morphology of the female and male gonads of these flies. In both sexes, only rudiments were found. In sim^{J1-47} females, tiny gonads developed that were generally not connected to the vulva. Despite the abnormal morphology, oogenesis apparently started normally, but arrested at an early stage (Figs. 6A″ and 6B″). This indicates that sim^{J1-47} does not affect the migration of the primordial germ cells into the developing gonads during embryogenesis. In males, only testis rudiments were found (Figs. 6C″ and 6D″).

Thus, the main defect in sim^{J1-47} flies raised at 17°C appeared to be due to defective genital disc development. The missing anus lead to a blind ending hindgut, whereas gut development itself was not severely affected and malpighian tubules form normally (Fig. 6D″). In addition, the gonads were not connected to the external excretory organs. Due to the lack of any opening, the gut swelled dramatically, which after a few days, lead to the death of the fly.

sim Affects Adult Behavior

To even further reduce the function of *sim* during development, we analyzed sim^{J1-47}/sim^{H9} animals. At 29°C, such flies never appeared, which was expected given the severe embryonic CNS phenotype (Fig. 1F). At 17°C, however, very rare escapers appeared (0.1% of the expected flies, the

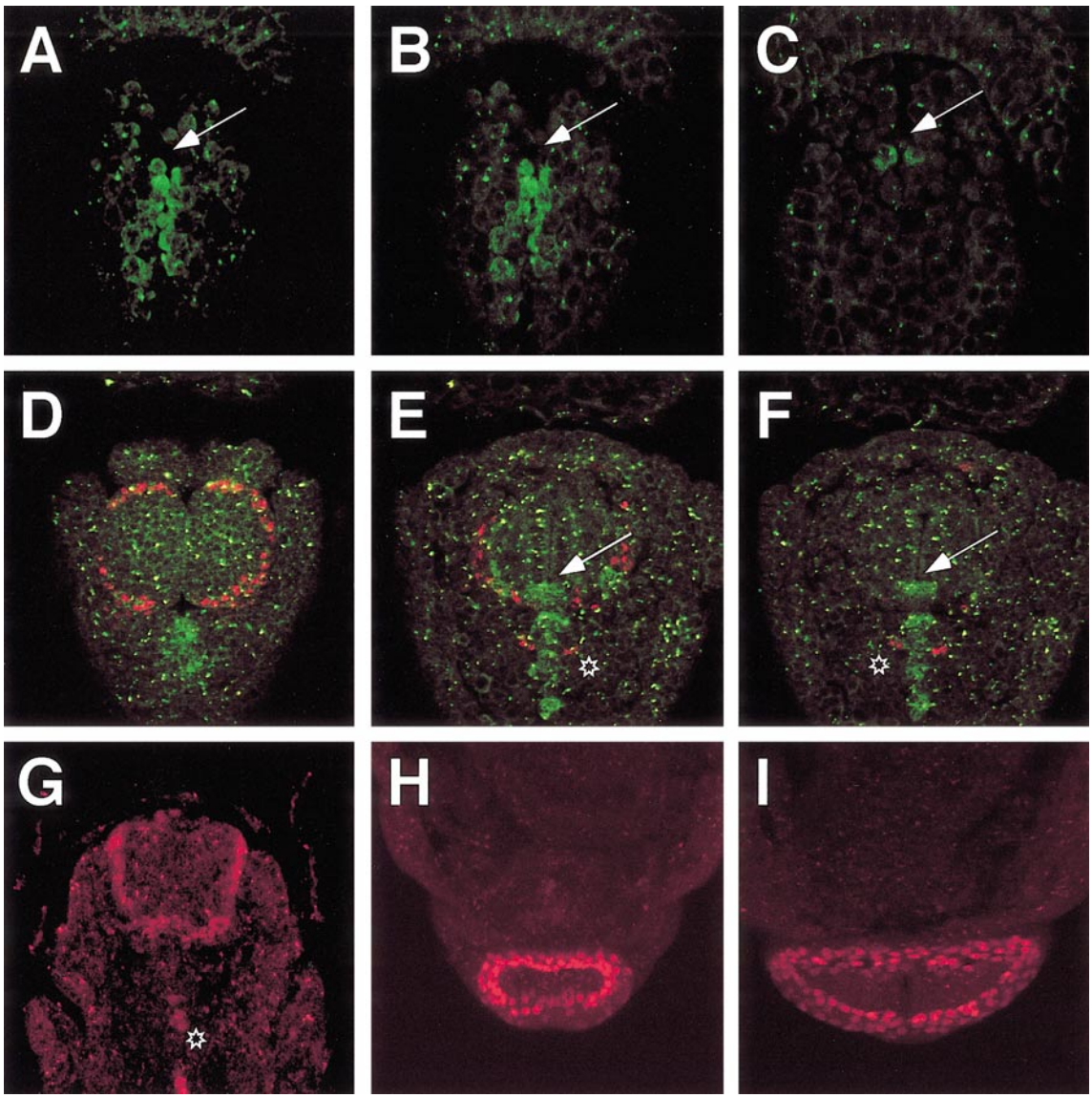

FIG. 4. Formation of the anal pad. The formation of the anal pad was followed by using anti-Eve antibodies and confocal microscopy. Sim expression (green) was detected by using anti-Sim antibodies. Mutant *sim* embryos (G, H) were recognized by the lack of Sim expression and the use of a labeled balancer chromosome. (A–C) Three consecutive focal planes from dorsal (A) to ventral (C) of a stage 8 embryo. Sim expression (green) extends to the posterior end of the germ band abutting the anterior end of the proctodeum. Arrows point to the proctodeum. (D–F) Three consecutive focal planes from dorsal (D) to ventral (F) of a stage 11/12 embryo. A crescent of Eve-expressing (red) cells is found at the posterior end of the germ band. At the ventral midline, Eve-expressing cells abut Sim-expressing cells; no coexpression is found. The Sim-expressing cells demarcate the anterior end of the proctodeum (arrow). (G) In *sim* mutant embryos (stage 11/12), Eve expression is found across the ventral midline. Abnormal formation of the proctodeum is already evident. (H) In stage 16 *sim* mutant embryos, the anal pad is reduced in size compared with wild type embryos (I). Asterisks indicate Eve-expressing neurons.

frequency depends on the exact culture conditions). These flies were sterile and frequently lacked external genitalia and the anal plate, similar to the phenotypes shown by homozygous mutant sim^{J1-47} flies. The sterility phenotype may be explained not only by defects in external and internal morphology, but also by misbehavior, as mutant males failed to perform the normal courtship behavior and mutant females ignored wild type males (only flies without external defects were examined).

In addition to abnormal courtship behavior, surviving sim^{J1-47}/sim^{H9} flies showed an extreme walking phenotype. The majority of the flies analyzed only walked in circles

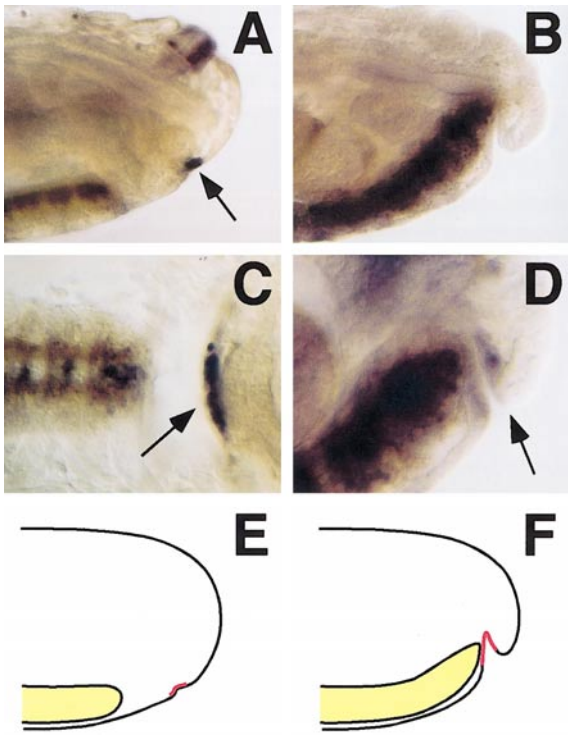

FIG. 5. Formation of the genital disc. Preparations of wild type (A, C) and mutant sim^{H9} (B, D) stage 16 embryos. The genital disc anlage has been labeled by Esg expression (arrows). Axons in the ventral nerve cord were visualized by using BP102 and subsequent HRP immunohistochemistry to determine the genotype. (A) In a lateral view, the genital disc anlage can be seen just anterior to the hindgut. (C) In dissected embryos, the disc cells are closely associated with the ectoderm. (E) Schematic drawing: the genital disc anlage is indicated in red. (B, D) In mutant *sim* embryos, Esg expression is initiated normally. However, in stage 16 embryos, a deep indentation (arrow) can be seen instead of an invaginated disc anlage. (F) Schematic drawing.

(see Figs. 7A–7D for walking traces). The phenotype was variable, possibly due to the changing levels of residual *sim* gene activity due to slight differences in the culture conditions. We further analyzed the behavioral deficits and studied 18 of these flies in Buridan's paradigm, which allows evaluation of many parameters of the flies' walking ability (Götz, 1980; Strauss and Heisenberg, 1993; Strauss and Pichler, 1998) (Fig. 7, and see Materials and Methods).

In Buridan's paradigm, wild type flies ran in relatively straight lines between the two stripes and show no preferred sense of rotation when they turned in front of the landmarks (Fig. 7E). Eleven sim^{J1-47}/sim^{H9} flies were tested in the first experiment; they generally turned either right or left (see Figs. 7A–7C for representative tracings). Interestingly, for a given fly, the turning direction usually did not change. Compared with wild type, all mutant flies showed a markedly reduced walking speed, and in most cases, the activity period was shorter (Figs. 7H and 7I). Only one of the *sim* flies showed some visible interest in the landmarks (see Fig. 7D).

In order to quantify a possibly existing residual orientation toward the landmarks, which might have been obscured by the circling behavior, the same individuals were monitored for an additional 15 min in the same arena but without landmarks. Normal flies then showed area-covering random search behavior with an increasing mean free path (Schuster and Götz, 1994). Again, sim^{J1-47}/sim^{H9} flies individually preferred either a clockwise or counterclockwise sense and, compared with wild type, showed reduced walking activity and speed (Figs. 7I and 7J). In Fig. 7F, the mean difference in orientation behavior between the Buridan behavior and random search behavior is shown for *sim* and wild type flies. Whereas wild-type flies showed the expected strong preference for the landmarks (i.e., small error angles are found more frequently than large error angles; see Materials and Methods), there was no detectable difference between Buridan and random search data in sim^{J1-47}/sim^{H9} flies. In summary, we find no measurable influence from visual landmarks on the orientation behavior of *sim* mutant flies.

We next addressed the important question whether sim^{J1-47}/sim^{H9} flies are blind by exposing them to optomotor stimuli. A striped drum consisting of six dark and six interspaced bright stripes rotated around the walking platform. All stripes were equally broad and equally spaced (i.e., pattern wavelength 60°; contrast 0.94; 30 full rotations were shown in 150 s). Wild-type flies turned in the sense of the pattern rotation in an attempt to compensate for the seen rotation (which is >90% under these conditions; Strauss *et al.*, 1997). In most *sim* flies, the spontaneous circling behavior was weakly modulated by the optomotor stimulus. Pattern rotation in their preferred direction enhanced their turning tendency, and stimulation against their preferred direction either decreased their turning tendency or even reversed it into the stimulus direction. For example, two spontaneously counterclockwise circling individuals showed 14 (16) counterclockwise rotations for 30 counterclockwise rotations of the pattern, whereas they performed 8 counterclockwise (2 clockwise) rotations for 30 rotations in the nonpreferred clockwise sense. Two of 11 inspected sim^{J1-47}/sim^{H9} flies did not react to optomotor stimuli at all. We thus conclude that most of the *sim* flies were not entirely blind.

The mean track length of sim^{J1-47}/sim^{H9} flies decayed significantly with every 3-min bin (Fig. 7G). Regardless of any landmarks, *sim* flies started out with about half the wild type track length and then walked progressively less. Wild type flies, in contrast, tended to produce a more constant track length, often over many hours, after their initial arousal from handling has decayed. Interestingly, females appeared to be affected more severely by the *sim* mutation. Detailed analysis of the walking traces using a laser carpet (Strauss, 1998) suggested that leg movement is coordinated normally; however, step length differs between the right and left body side (data not shown).

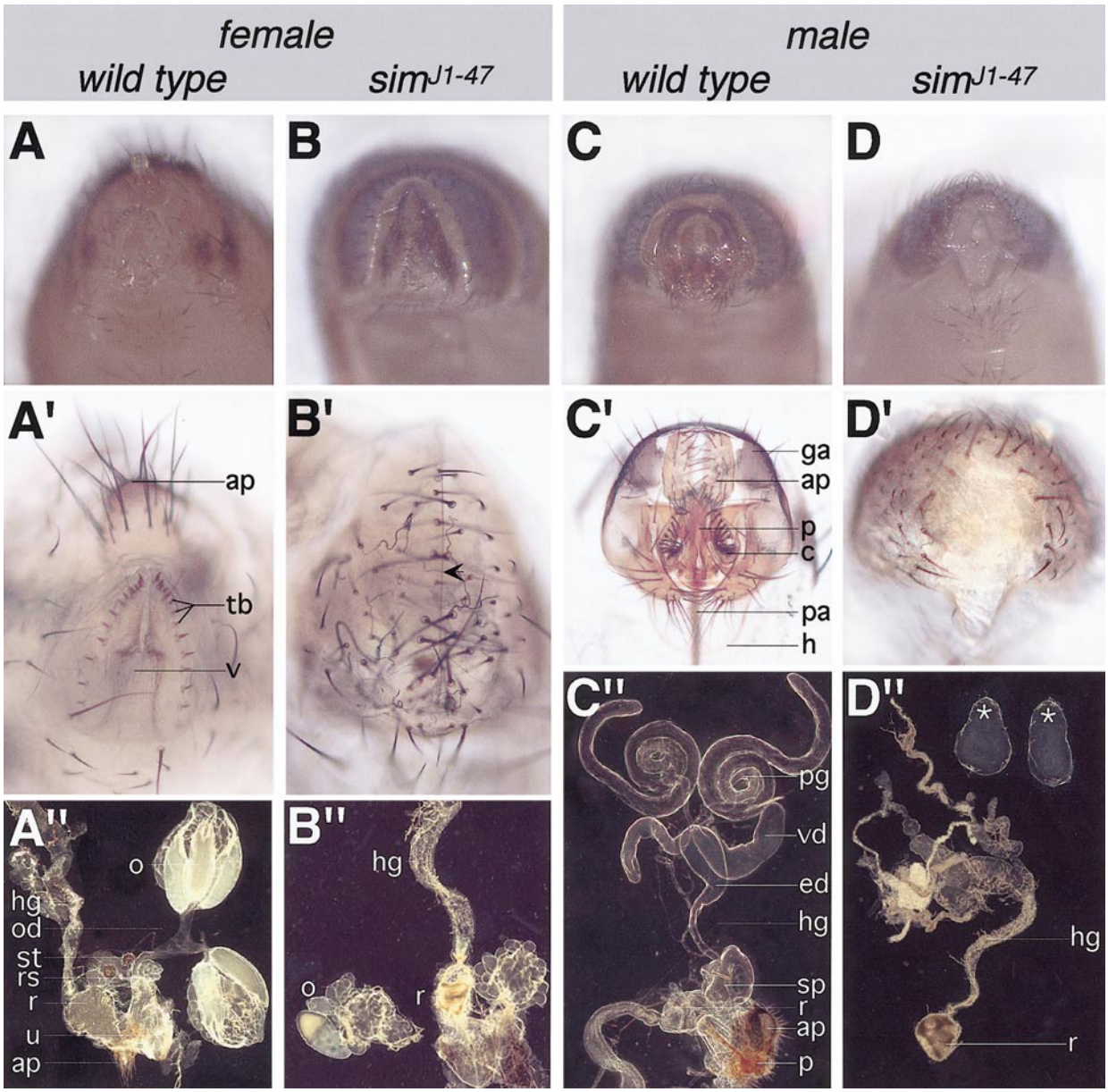

FIG. 6. Adult phenotypes associated with *sim*. Preparations of wild type and mutant *sim* flies. The tail regions and the gonads are shown. (A, A′) *Drosophila* wild type females can be easily recognized by the prominent anal pad (ap) and the thorn bristles (tb) around the vulva (v). (B, B′) In homozygous mutant sim^{J1-47} females, the anal plate cannot be recognized. The thorn bristles and the vulva appear to be missing. (A″) Wild type ovaries. The ovaries (o) are well developed and are connected via the oviduct (od) and the uterus (u) to the vulva [hindgut (hg); rectum (R); spermathecae (st); seminal receptacle (rs)] (B″) In mutant sim^{J1-47} female flies, the ovaries are present although poorly developed. Oogenesis apparently starts normally but stops prematurely. The hindgut is not connected to the rectum (r) and is frequently swollen. (C, C′) Wild type males have a flat anal plate (ap) and a dark pigmented clasper (c) surrounding the penis apparatus (p). (D, D′) In homozygous mutant sim^{J1-47} males, the anal plate, the clasper, and the penis are missing. (C″) In wild type males, the testis is well developed. Paragonium (pg), vas deferens (vd), ejaculatory duct (ed), and sperm pump (sp) can be detected. (D″) In homozygous mutant sim^{J1-47} males, testis development is severely impaired. Only rudiments (asterisk) that are not connected to the outside are found. As in females, the hindgut (hg) is not properly connected to the rectum (r).

Histological Analyses of sim^{ts} Animals

Consistent with the behavioral defects, we noted alterations in the normal brain structure. Serial frontal sections were examined for all of the sim^{J1-47}/sim^{H9} flies in which behavior was assessed. The series were inspected by using autofluorescence conditions under which all neuropil have a blue–green and the pericarya a bright green to yellow

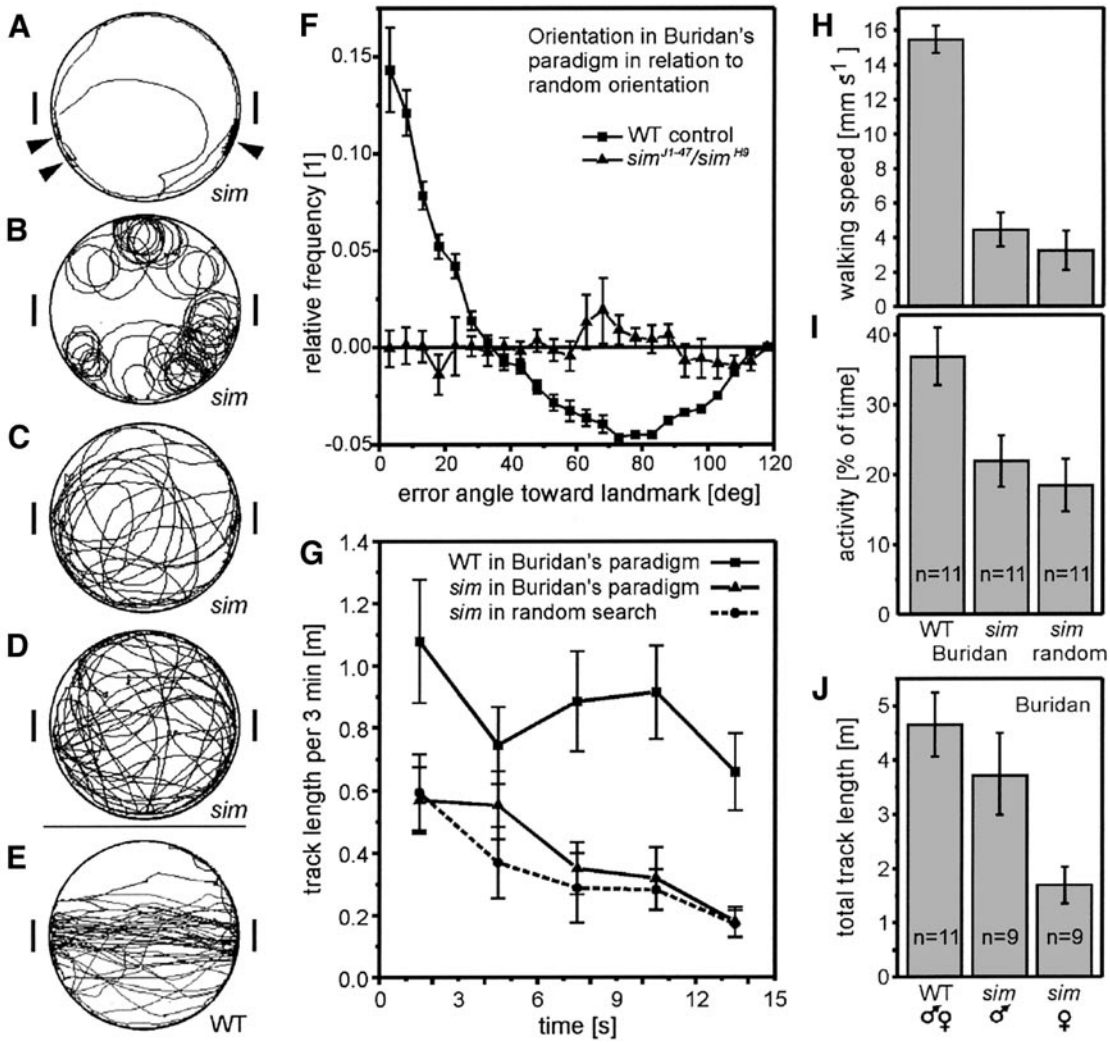

FIG. 7. Walking and orientation behavior phenotype. (A–E) Walking traces. Single flies walked for 15 min on an elevated water-surrounded platform of 85 mm diameter. sim^{J1-47}/sim^{H9} flies walk in circles (A–D) despite the two inaccessible landmarks (indicated by the vertical bars) which keep wild type flies alternating between them for many hours (E, wild-type: Oregon-R). sim^{J1-47}/sim^{H9} flies have a preferred side to which they almost always turn. (A) Five-minute walking traces from an extremely tight turning *sim* fly (arrowheads point to very high frequency turning points). (B, C) Medium wide and a wide turning mutant *sim* fly. (D) Exceptional example of a sim^{J1-47}/sim^{H9} fly producing a measurable orientation component toward the landmarks. (F) Mean occurrence frequency of certain error angles between the actual walking direction (obtained every 0.2 s) and the straight direction toward the nearer, in angular terms, of the two landmarks (Buridan's paradigm) minus the respective frequency distribution for random search behavior in the absence of landmarks. $N = 11$ flies per test group (sim^{J1-47}/sim^{H9}, wild type Oregon-R) were measured in random order each for 15 min in the Buridan situation and for 15 min in the empty arena. On average, there is no measurable influence from the landmarks on the orientation behavior of mutant *sim* flies. (G) Mean track length per 3-min bin. Same experimental groups as in (F). Regardless of the presence or absence of landmarks, *sim* mutant flies start with about half the wild-type track length and decay significantly, whereas wild type flies tend to produce a more constant track length as soon as their initial arousal from handling has decayed. The overall deficits in the track length of mutant *sim* flies are due to a drastically reduced walking speed (H) and to a bisected activity (I; mean percentage of time spent walking). (J) Mutant *sim* female flies are more strongly affected than mutant *sim* male flies. An insignificantly lower walking speed and lower activity in females combine to a significant deficit in mean walked distance when compared with male *sim* flies (*t*-test, two-tailed: $P < 0.05$). All error bars indicate SEMs.

appearance (Fig. 8). In particular, we noted defects associated with the inner chiasm of the optic lobes and in the central complex (CX), a structure that spans the protocerebral hemispheres and develops from the larval interhemispheric commissure during larval and pupal stages (Hanesch *et al.*, 1989). The CX is composed of the four

neuropilar regions called the protocerebral bridge (pb), fan-shaped body (fb), ellipsoid body, and paired noduli. In 70% of the 19 inspected *sim* brains, the pb as the posterior-most CX neuropil was markedly thinner at the sagittal midplane and generally less compact than the intact wild type pb (Figs. 8A and 8B). The pb consists of a linear array of 8 bilaterally paired glomeruli. Fibers might be missing in *sim* flies, which normally run along the pb and connect the paired glomeruli in a highly ordered fashion (Hanesch *et al.*, 1989). The fb, the largest of the CX neuropils, was divided sagittally in its posterior shell in 15% of the *sim* brains (Figs. 8C and 8D). The ellipsoid-body and noduli were not affected by the *sim* mutation.

The inner chiasm of the optic lobes connects the medulla with the lobula and the lobula plate. In 40% of the inspected *sim* flies, ectopic fiber bundles were found to cut into the lobula either unilaterally or bilaterally (Figs. 8E and 8F). Such ectopic bundles are never observed in wild-type optic lobes (Brunner *et al.*, 1992). We were unable to directly correlate the gross anatomical salience of the CX or optic lobe defects with the severity of the walking problems or the degree of circling. Flies with a unilateral inner chiasm defect circled as consistently as flies with no visible defect. As an exception, one of the putatively blind flies mentioned above had the most severe optic lobe defects on both sides.

Postembryonic Expression of sim in the CNS

The above described phenotypes suggest that *sim* is expressed postembryonically. This was initially examined by RT-PCR experiments (see Materials and Methods), which demonstrated that *sim* transcripts were present throughout fly development (Fig. 9). Transcripts were barely detected in whole third instar larvae, but were abundant in dissected larval brains (Fig. 9).

Spatial expression of Sim was further examined by immunostaining larvae and adult flies with Sim antibodies, followed by examination with confocal microscopy. In the larval ventral nerve cord, *sim* is expressed in the midline glial cells (Fig. 10A). These cells, which can easily be identified by their characteristic morphology (Awad and Truman, 1997; Stollewerk *et al.*, 1996), express Sim during embryonic CNS development (Crews *et al.*, 1988; Thomas *et al.*, 1988).

Similar to its distribution in embryonic cells, Sim protein was confined to cell nuclei (Ward *et al.*, 1998). During embryonic development, nuclear localization of the Sim protein requires heterodimerization with the Tgo bHLH-PAS protein. Tgo is found in all cells and is localized to the cytoplasm in the absence of a partner bHLH-PAS protein, such as Sim (Ward *et al.*, 1998). In the presence of Sim, the Sim:Tgo complex translocates to the nucleus, and immunostaining with Anti-Tgo shows prominent nuclear staining in those cells. To analyze whether Sim may interact with Tgo in the larval midline cells and to obtain a validation control for the Sim immunostaining, we double-stained larval nerve cords with anti-Sim and anti-Tgo antibodies. The results revealed a complete colocalization of nuclear Sim and Tgo expression in the CNS midline (Fig. 10C).

Examination of larval brain staining revealed additional sites of Sim localization. Sim was prominently expressed in the lamina and the medulla, which are synaptic targets of photoreceptor axons (Fig. 10D). Again, a colocalization of Tgo was found (Figs. 10E and 10F). Examination of the central brain, which has been implicated in the control of the walking behavior, identified two clusters of Sim-positive cells, one on each side of the midline (Figs. 10I and 10J). Each cluster has three groups of cells that are not contiguous. The two anterior-most clusters showed higher levels of Sim protein than the posterior-most cluster (Fig. 10J). These cells may be important for the locomotor defects of mutant sim^{J1-47}/sim^{H9} flies. Despite the fact that sim^{J1-47}/sim^{H9} flies are probably able to see (see above), Sim expression in the optic lobe might nevertheless contribute to the behavioral deficits. There also exist smaller, less distinct, groups of Sim-expressing cells in the anterior of the brain (not shown).

Thus, the temporal and spatial expression pattern of *sim* support a postembryonic function of the gene. The availability of the temperature-sensitive *sim* allele could in principle be used to address this question. However, since only very few sim^{J1-47}/sim^{H9} flies eclosed even at the permissive temperature, we could only analyze sim^{J1-47}/sim^{J1-47} flies. Flies were crossed at the permissive temperature of 17°C and were transferred to fresh food vials every 24 h. The animals were subjected to the restrictive temperature (29°C) in 24-h intervals. As long as the shift to the restrictive temperature occurred after embryogenesis, normal numbers of flies eclosed, indicating that postembryonic functions of *sim* do not affect viability.

DISCUSSION

The gene *sim* acts as a master regulatory gene controlling midline development in the ventral nerve cord of *Drosophila*. In fact, it was one of the first genes associated with such an important function during cell-type specification. The function of *sim* outside the nerve cord has been known for a long time but was never investigated in much detail. Here, we report the identification of a temperature-sensitive *sim* mutation that demonstrates a requirement of *sim* during genital imaginal disc and anal pad development. In addition, behavioral deficits are associated with *sim* function. Most importantly, we noted a walking defect that is likely due to a disruption of the central brain complex development in conjunction with a developmental defect found in the inner chiasm of the optic lobes.

Embryonic Function of sim

sim expression is first evident during the cellular blastoderm stage in a strip of cells flanking the mesodermal

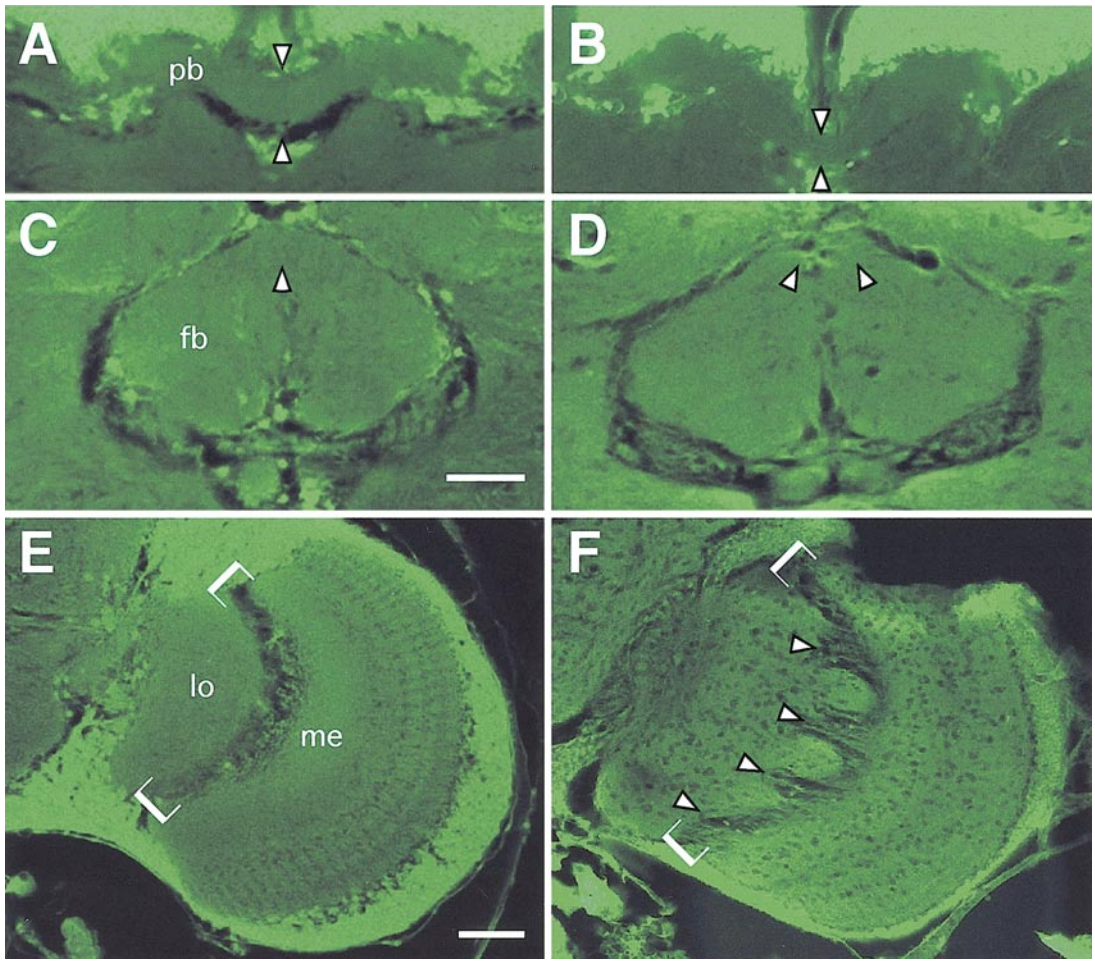

FIG. 8. Structural defects in the adult *sim* brain. Frontal 7-μm-thick sections through wild type brains (A, C, E) and sim^{J1-47}/sim^{H9} brains at comparable levels (B, D, F). Dorsal is up. Under autofluorescence conditions, all neuropil appears in darker green and the pericarya in bright green–yellow. (A, B) In 70% of the inspected *sim* brains, the protocerebral bridge (pb) of the central complex was markedly thinner and less compact than a wild type pb. Arrowheads indicate the thinnest part at the sagittal midplane. (C, D) The fan-shaped body (fb) of the central complex was divided posterior–sagittally in 15% of the *sim* brains. Arrowheads indicate the dorsal-most extents of the fb. (E, F) The inner chiasm of the optic lobes (only right side is shown) is situated between the medulla (me) and the lobula (lo). The ventral and dorsal ends of the chiasm region are indicated by open brackets. The inner chiasm was disordered either unilaterally or bilaterally in 40% of the *sim* brains. Axon bundles take an abnormal path into the distal lobula, cutting into this neuropil to varying depths (arrowheads). Such bundles are never observed in wild type optic lobes. Scale bars indicate 20 μm; (A–D) are on the same scale as (C); the bar in (E) applies also to (F).

anlage. The majority of these cells will later divide to generate the neurons and glial cells found at the midline of the ventral nerve cord. It is important to note, however, that *sim* expression exceeds the neurogenic region from which the nerve cord will form. At the posterior, *sim* expression extends into abdominal segment 10, where it can be detected until end of stage 11. The fate of these cells is presently unknown. Possibly, the ectodermal midline cells provide inductive signals influencing the developing neighboring tissues, which appears to be a more general feature of the midline cells. Within the CNS, the midline cells act as an organizing center controlling the patterning of axons by providing attractive and repulsive cues. Furthermore, the midline cells regulate the number and differentiation of cortical neurons and mesodermal cells (Chang *et al.*, 2000; Lüer *et al.*, 1997; Menne *et al.*, 1997; Zhou *et al.*, 1997).

The anal pad anlage can be labeled by Eve expression (Gorfinkiel *et al.*, 1999) and forms immediately posterior to Sim-expressing cells. In *sim* mutants, the Eve expression domain shifts toward the midline and meets at the midline. Possibly, the gap in Eve expression in wild type embryos allows the formation of the anal slit. In *sim* mutants, the posterior midgut invaginates normally and the proctodeum initially forms. However, during later stages, the cells that

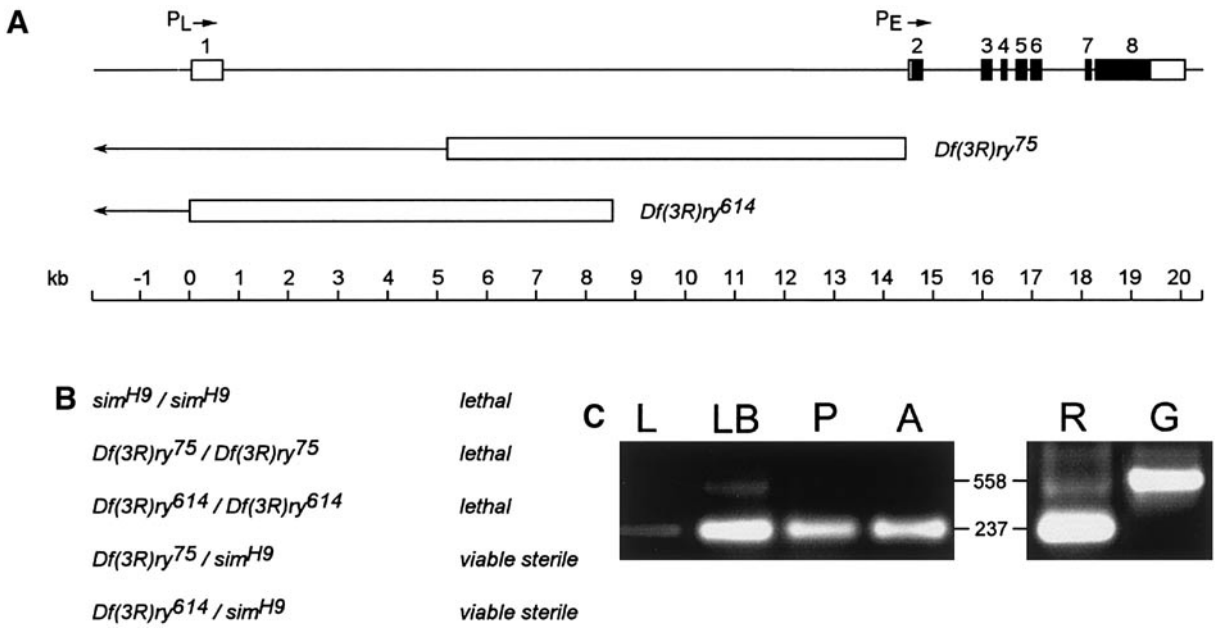

FIG. 9. Postembryonic expression of *sim*. (A) The schematic depicts the *sim* gene structure. Exons are numbered 1–8 with untranslated regions shown as unfilled boxes and the coding sequence depicted as filled boxes. The early promoter (P_E) drives expression in the CNS midline precursor cells, whereas the late promoter (P_L) drives expression in embryonic midline glia. Two deletions, $Df(3R)ry^{75}$ and $Df(3R)ry^{614}$, remove P_L, but leave early expression intact. The breakpoints of the deletions are within the boxed regions and DNA to the left of the box is deleted. Scale in kb is shown at the bottom. (B) Flies that are either $Df(3R)ry^{75}/sim^{H9}$ or $Df(3R)ry^{614}/sim^{H9}$ presumably have sufficient embryonic *sim* expression for viability. However, the resulting male and female adults are sterile. (C) RT-PCR was carried out on total RNA from different *Drosophila* stages, including 0- to 18-h embryos (E), third instar larvae (L), dissected third instar larval brains (LB), pupae (P), and adults (A). Total RNA was converted to cDNA by using a gene-specific primer and reverse transcriptase. PCR was performed by using a primer pair corresponding to the *sim* coding sequence. After PCR, the DNA products were electrophoresed on an agarose gel and visualized by ethidium bromide staining. The primer pair spanned an intron, so that the predicted size of the mRNA amplification product is 237 bp and the predicted size of the amplification product from genomic DNA is 558 bp. This is confirmed by *in vitro* transcribing a *sim* cDNA clone, followed by RT-PCR and electrophoresis. The 237-bp product is shown (R). Amplification of *Drosophila* genomic DNA shows the 558-bp predicted band (G). The presence of a 237-bp product in the developmentally staged RNA lanes indicates that the amplification product is derived from RNA and not from contaminating genomic DNA.

will give rise to the anus will die and thus prevent the external opening of the hindgut.

What is the function of the ventral midline during genital disc development? In both female and male flies, the sexually dimorphic terminalia are formed by a common genital disc comprising three primordia (Sanchez and Guerrero, 2001). The female genital primordium is derived from the 8th abdominal segment, the male genital primordium from the 9th abdominal segment, and the anal primordium from the 10th and 11th abdominal segments. In both sexes, the anal primordium will develop, whereas depending on the sex of the animal, either the female or the male primordium will develop (Sanchez and Guerrero, 2001). The definition of the genital disc anlage does not appear to be affected in *sim* mutants, but the subsequent delamination from the ectoderm is abnormal. In wild type embryos, the genital disc anlage forms just posterior to the developing ventral nerve cord. Following germ band retraction, the ventral nerve cord retracts, and concomitantly, the genital disc anlage delaminates from the ectoderm. At present, our analyses do not allow us to discriminate whether the genital disc phenotype found in mutant *sim* embryos is an indirect consequence of the nerve cord condensation defect or whether it is due to the loss of *sim* expression in the genital disc primordium.

sim Function during Adult Stages

The temperature-sensitive mutation sim^{J1-47} allowed us to address the question whether *sim* is required in larval or adult stages. Following the reduction of *sim* function, a number of interesting phenotypes emerged. The sterility phenotype displayed by the hypomorphic *sim* allele *J1–47* as well as the amorphic mutation sim^{H9} in trans to deficiencies affecting only one of the two promoters (Fig. 8) demonstrated that these phenotypic traits are indeed due to a reduction in the level of *sim* function. The sterility phenotype is likely to be a direct consequence of abnormal genital

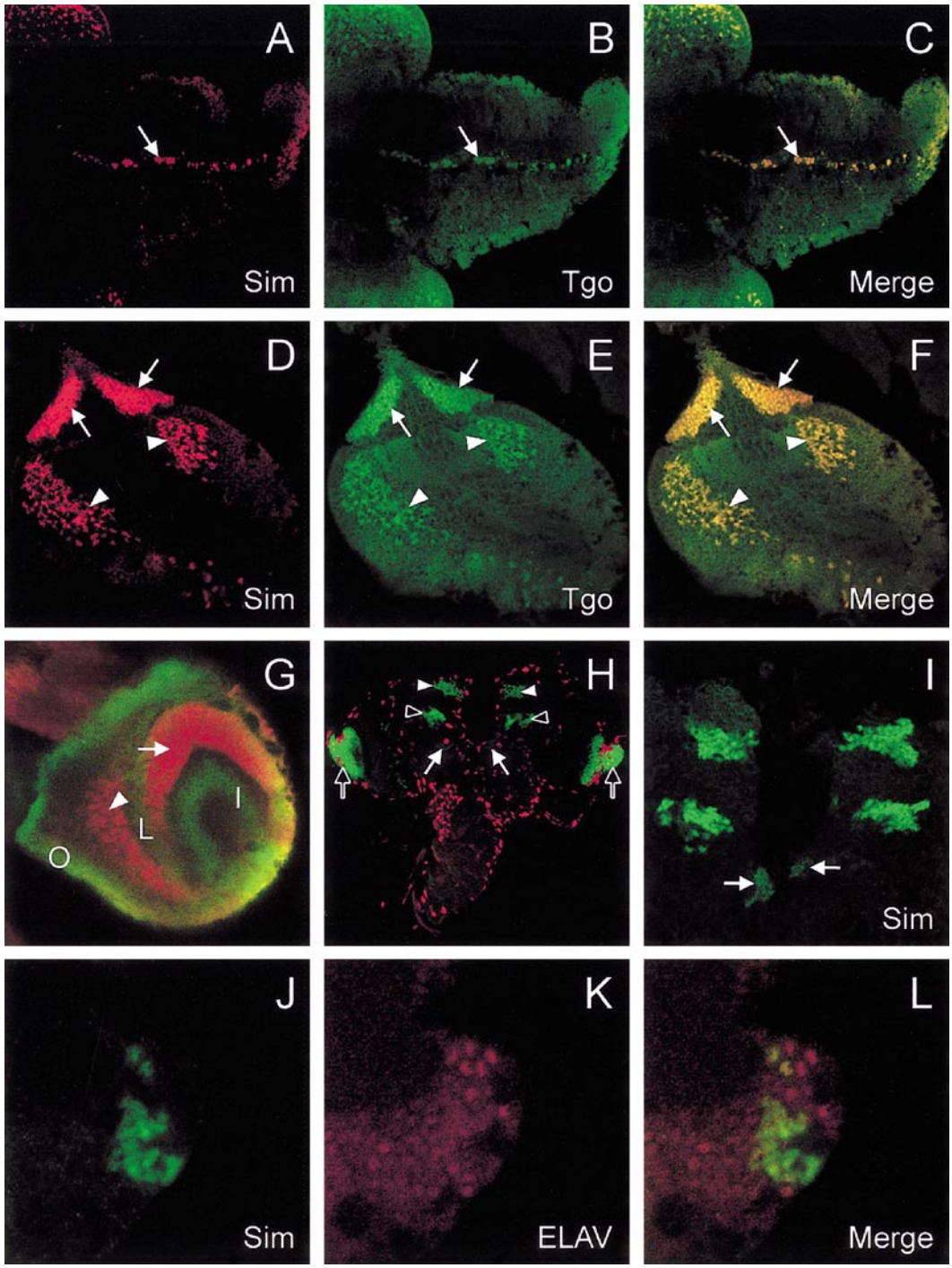

FIG. 10. Sim protein expression in the larval CNS. Third instar larval brains and ventral nerve cord (vnc) were dissected from third instar larvae, stained with antibodies, and examined by confocal microscopy. (A–C) Larval CNS was double-stained with anti-Sim (A; red) and anti-Tgo (B; green). Merge image is shown in (C). Horizontal view of the dorsal surface of the vnc is shown. (A) Sim is found in nuclei of cells that lie along the midline of the vnc (arrow). (B) Tgo is present in the cytoplasm of all vnc cells, but accumulates in nuclei of only the midline cells (arrow). (C) Merge image shows overlap of Sim and Tgo nuclear staining in the midline cells (arrow). (D–F) Dissected optic lobe of larval brain double-stained with anti-Sim (D) and anti-Tgo (E). Merge image is shown in (F). (D) Nuclear Sim staining is observed in cells of the lamina (arrows) and medulla (arrowheads). (E) Tgo is present in the nuclei of the lamina (arrows) and medulla (arrowheads) and present in the cytoplasm elsewhere. (F) The merge image shows that nuclear Sim and Tgo completely overlap. (G) Optic lobe from a PCNA-GFP larva stained with anti-Sim (red) and visualized for GFP (green). The GFP is expressed in the proliferation centers of the optic lobe, including

disc development during embryonic stages. Interestingly, these flies also showed abnormal courtship behavior, suggesting a requirement of *sim* in larval/adult neurogenesis. A similar conclusion has to be drawn by the walking defects of mutant *sim* flies. Mutant flies were only able to walk in circles. This phenotype could be due to a loss of motoneurons in the ventral nerve cord or it could be due to disruption of higher centers that coordinate walking.

An extended analysis of the walking behavior in different structural brain mutants showed that the central complex (CX) between the protocerebral brain hemispheres serves as such a higher center (Heisenberg and Böhl, 1979; Strauss and Heisenberg, 1993). A hallmark of mutants affecting the CX was a slower mean and maximum walking speed and a decaying locomotor activity in Buridan's paradigm, which is also shown by sim^{J1-47}/sim^{H9} flies. In the majority of these mutants, the protocerebral bridges and their fan-shaped bodies were affected. The remaining flies with no gross morphological CX defects may well have defects that may be detectable only at the single cell level.

Why do sim^{J1-47}/sim^{H9} flies circle? First of all, circling in only one direction is not the normal behavior of blind flies in the arena situation. They would show random-search behavior with a balanced frequency of left and right turns (e.g., *no-receptor-potential* A^{P24}; data not shown). Secondly, we assume that most *sim* flies are not entirely blind since most of them reacted, at least weakly, to optomotor stimuli. *sim* flies are not the first example of circling flies. In the screen for locomotor mutants, the CX-defective mutant *C31* was isolated that frequently walked in wavy lines (Strauss and Trinath, 1996). *C31* function was subsequently studied in mosaics that were generated by using the gynandromorph technique. When one half of the body, including the head, was mutant, the flies were unable to walk straight and persistently turned toward the defective body side. However, unilateral mutant flies with an intact brain could walk straight pointing toward the role of the CX in balancing left–right motocontrol (Strauss and Trinath, 1996; R.S., unpublished observation). In support of the notion that the CX controls locomotive behavior is the finding that *Pax-6/eyeless* mutants cause gross morphological CX defects and, concomitantly, severe locomotor deficits (Callaerts *et al.,* 2001).

A mutation in the gene *pirouette,* which was identified in a screen for genes affecting auditory behavior, shows a similar walking phenotype as described here for the hypomorphic *sim* mutation (Eberl *et al.,* 1997). Within the CNS, the optic lobes degenerate but no information about the development of the CX is available. We have not observed any genetic interaction between the two loci (data not shown). To date, only few other mutations have been described that specifically affect the development of the CX. The transcription factor AP2 is not required during embryonic development; however, adult flies display severe disruptions in the CX. It is unknown whether AP2 mutations affect behavior similar to *sim* (Monge *et al.,* 2001). Other mutants affecting the formation and connectivity of the CX have been described, but no information is available on walking abilities of the different mutant flies (Boquet *et al.,* 2000; Hitier *et al.,* 2001; Simon *et al.,* 1998).

Beside expression within the central complex, we noted high levels of Sim expression in the optic lobes, the lamina, and the medulla, which is in agreement with the mutant phenotype. During larval development, the optic lobes undergo extensive rounds of cell proliferation to give rise to the mature neurons and glia. DNA replication and cell division occur at several discrete sites: the inner proliferative center (IPC), the outer proliferative center (OPC), and the laminar precursor center (LPC) (Hofbauer and Campos-Ortega, 1990; Selleck and Steller, 1991). Since *sim* expression was observed during the proliferative phase of optic lobe development, we addressed whether *sim* was expressed in proliferating cells or the postmitotic cells. The proliferative zones were visualized by expression of GFP from a PCNA-GFP transgenic strain (R. Duronio, personal communication). The *Drosophila* Proliferating Cell Nuclear Antigen (PCNA) gene is encoded by the *mus209* locus and is expressed in replicating cells. Since PCNA-GFP and Sim expression do not overlap (Fig. 10G), it appears that Sim is only expressed in postmitotic cells in the optic lobes. Double labeling experiments with glial and neuronal antigens indicate that, within the brain, Sim is expressed only in neuronal cells (Figs. 10J–10L). The optic lobes of *sim* mutant flies show aberrant axonal projects, but the medullary and laminar neurons are present. This suggests that the role of *sim* in optic lobe development may be different from its role in controlling formation of the CNS midline cells in embryonic development.

---

outer proliferation center (O), lamina precursor center (L), and inner proliferation center (I). Sim protein is shown in the lamina (arrow) and medulla (arrowhead). There is no overlap between the GFP and Sim expression, indicating that Sim is not expressed in proliferating cells of the optic lobe. (H) Brain from a *repo-lacZ* third instar larva double-stained with anti-Sim (green) and anti-β-gal (red). The *repo-lacZ* enhancer trap line expresses *lacZ* in glia. Sim expression is observed in the lamina (unfilled arrows) and three paired regions in the central brain complex (arrowheads). The two most anterior clusters (filled and unfilled arrowheads) stain more intensely than the most posterior clusters (filled arrow). The Sim-positive cells in the central complex are nonglial, since they do not overlap with *repo-lacZ*-expressing glial cells. (I) Higher magnification of the Sim-expressing central brain clusters showing the three paired clusters. (J–L) Central brain Sim-positive cells are neuronal. Larval brain was double-stained with anti-Sim (J; green) and anti-ELAV (K; red). Merge is shown in (L). ELAV is specifically expressed in postmitotic neurons. The Sim-positive cells are also ELAV-positive.

ACKNOWLEDGMENTS

We thank R. Nöthiger for advice and help, John Nambu who carried-out early experiments on *sim* sterile phenotypes, Mary Ward who performed initial Sim larval brain staining, D. Eberl for mutant *pirouette* flies, C. S. Goodman for antibodies, Bob Duronio, Craig Montell, and Andrew Tomlinson for advice and reagents, and members of the Klämbt lab for help and discussions. This work was supported through a predoctoral fellowship of the Boehringer Ingelheim Fonds (to J.P.), a BMBF-BioFuture grant (to R.S.), a grant from NICHD (to S.T.C.), and a grant of the DFG (to C.K.).

REFERENCES

Ashburner, M. (1989). "Drosophila: A Laboratory Manual." Cold Spring Harbor Laboratory Press, Cold Spring Harbor, NY.

Awad, T. A., and Truman, J. W. (1997). Postembryonic development of the midline glia in the CNS of Drosophila: Proliferation, programmed cell death, and endocrine regulation. *Dev. Biol.* **187,** 283–297.

Bashaw, G. J., and Goodman, C. S. (1999). Chimeric axon guidance receptors: The cytoplasmic domains of slit and netrin receptors specify attraction versus repulsion. *Cell* **97,** 917–926.

Boquet, I., Hitier, R., Dumas, M., Chaminade, M., and Preat, T. (2000). Central brain postembryonic development in Drosophila: Implication of genes expressed at the interhemispheric junction. *J. Neurobiol.* **42,** 33–48.

Bossing, T., and Technau, G. M. (1994). The fate of the CNS midline progenitors in Drosophila as revealed by a new method for single cell labeling. *Development* **120,** 1895–1906.

Brose, K., and Tessier-Lavigne, M. (2000). Slit proteins: Key regulators of axon guidance, axonal branching, and cell migration. *Curr. Opin. Neurobiol.* **10,** 95–102.

Brunner, A., Wolf, R., Pflugfelder, G. O., Poeck, B., and Heisenberg, M. (1992). Mutations in the proximal region of the optomotor-blind locus of *Drosophila melanogaster* reveal a gradient of neuroanatomical and behavioral phenotypes. *J. Neurogenet.* **8,** 43–55.

Callaerts, P., Leng, S., Clements, J., Benassayag, C., Cribbs, D., Kang, Y. Y., Walldorf, U., Fischbach, K. F., and Strauss, R. (2001). Drosophila Pax-6/eyeless is essential for normal adult brain structure and function. *J. Neurobiol.* **46,** 73–88.

Campos-Ortega, J. A., and Hartenstein, V. (1997). "The Embryonic Development of *Drosophila melanogaster.*" Springer-Verlag, Berlin.

Chang, J., Kim, I. O., Ahn, J. S., Kwon, J. S., Jeon, S. H., and Kim, S. H. (2000). The CNS midline cells coordinate proper cell cycle progression and identity determination of the Drosophila ventral neuroectoderm. *Dev. Biol.* **227,** 307–323.

Crews, S. T. (1998). Control of cell lineage specific development and transcription by bHLH PAS proteins. *Genes Dev.* **12,** 607–620.

Crews, S. T., Thomas, J. B., and Goodman, C. S. (1988). The Drosophila single-minded gene encodes a nuclear protein with sequence similarity to the per gene product. *Cell* **52,** 143–151.

Eberl, D. F., Duyk, G. M., and Perrimon, N. (1997). A genetic screen for mutations that disrupt an auditory response in Drosophila melanogaster. *Proc. Natl. Acad. Sci. USA* **94,** 14837–14842.

Emmons, R. B., Duncan, D., Estes, P. A., Kiefel, P., Mosher, J. T., Sonnenfeld, M., Ward, M. P., Duncan, I., and Crews, S. T. (1999). The spineless-aristapedia and tango bHLH-PAS proteins interact to control antennal and tarsal development in Drosophila. *Development* **126,** 3937–3945.

Escherich, K. (1902). Zur Entwicklung des Nervensystems der Musciden, mit besonderer Berücksichtigung des sog Mittelstranges. *Zeitschrift für Wissensch. Zoologie* **LXXI,** 525–549.

Estes, P., Mosher, J., and Crews, S. T. (2001). Drosophila single-minded represses gene transcription by activating the expression of repressive factors. *Dev. Biol.* **232,** 157–175.

Ferre-D'Amare, A. R., Prendergast, G. C., Ziff, E. B., and Burley, S. K. (1993). Recognition by Max of its cognate DNA through a dimeric b/HLH/Z domain. *Nature* **363,** 38–45.

Foe, V. E. (1989). Mitotic domains reveal early commitment of cells in Drosophila embryos. *Development* **107,** 1–22.

Gorfinkiel, N., Sanchez, L., and Guerrero, I. (1999). Drosophila terminalia as an appendage-like structure. *Mech. Dev.* **86,** 113–123.

Götz, K. G. (1980). Visual guidance in Drosophila. In "Development and Neurobiology of Drosophila" (O. Siddiqui, P. Babu, L. M. Hall, and J. C. Hall, Eds.), pp. 391–407. Plenum Press, New York.

Hanesch, U., Fischbach, K.-F., and Heisenberg, M. (1989). Neuronal architecture of the central complex in *Drosophila melanogaster*. *Cell Tissue Res.* **257,** 343–366.

Hartenstein, V., and Jan, Y. N. (1992). Studying Drosophila embryogenesis with P-lacZ enhancer trap lines. *Roux's Arch. Dev. Biol.* **201,** 194–220.

Hayashi, S., Hirose, S., Metcalfe, T., and Shirras, A. D. (1993). Control of imaginal cell development by the escargot gene of Drosophila. *Development* **118,** 105–115.

Heisenberg, M., and Böhl, K. (1979). Isolation of anatomical brain mutants of Drosophila by histological means. *Z. Naturforsch.* **34c,** 143–147.

Hitier, R., Chaminade, M., and Preat, T. (2001). The Drosophila castor gene is involved in postembryonic brain development. *Mech. Dev.* **103,** 3–11.

Hofbauer, A., and Campos-Ortega, J. A. (1990). Proliferation pattern and early differentiation of the optic lobes in Drosophila melanogaster. *Roux's Arch. Dev. Biol.* **198,** 264–274.

Hummel, T., Schimmelpfeng, K., and Klämbt, C. (1997). Fast and efficient egg collection and antibody staining from large numbers of *Drosophila* strains. *Dev. Genes Evol.* **207,** 131–135.

Hummel, T., Schimmelpfeng, K., and Klämbt, C. (1999). Commissure formation in the embryonic CNS of *Drosophila*. I. Identification of the required gene functions. *Dev. Biol.* **208,** 381–398.

Jacobs, J. R. (2000). The midline glia of Drosophila: A molecular genetic model for the developmental functions of Glia. *Prog, Neurobiol,* **62,** 475–508.

Jürgens, G., and Hartenstein, V. (1993). The terminal regions of the body pattern. In "Development of Drosophila" (C. M. Bate and A. Martinez-Arias, Eds.), Vol. 1, pp. 687–746. Cold Spring Harbor Laboratory Press, Cold Spring Harbor, NY.

Kidd, T., Bland, K. S., and Goodman, C. S. (1999). Slit is the midline repellent for the robo receptor in Drosophila. *Cell* **96,** 785–794.

Kinrade, E. F., Brates, T., Tear, G., and Hidalgo, A. (2001). Roundabout signalling, cell contact and trophic support confine longitudinal glia and axons in the Drosophila CNS. *Development* **128,** 207–216.

Klämbt, C., Jacobs, J. R., and Goodman, C. S. (1991). The midline of the Drosophila central nervous system: A model for the genetic analysis of cell fate, cell migration, and growth cone guidance. *Cell* **64,** 801–815.

Kramer, S. G., Kidd, T., Simpson, J. H., and Goodman, C. S. (2001). Switching repulsion to attraction: Changing responses to slit during transition in mesoderm migration. *Science* **292,** 737–740.

Lewis, J. O., and Crews, S. T. (1994). Genetic analysis of the Drosophila single minded gene reveals a central nervous system influence on muscle development. *Mech. Dev.* **48,** 81–91.

Lüer, K., Urban, J., Klämbt, C., and Technau, G. M. (1997). Induction of identified mesodermal cells by CNS midline progenitors in Drosophila. *Development* **124,** 2681–2690.

Ma, Y., Certel, K., Gao, Y., Niemitz, E., Mosher, J., Mukherjee, A., Mutsuddi, M., Huseinovic, N., Crews, S. T., Johnson, W. A., and Nambu, J. R. (2000). Functional interactions between Drosophila bHLH/PAS, Sox, and POU transcription factors regulate CNS midline expression of the slit gene. *J. Neurosci.* **20,** 4596–4605.

Mayer, U., and Nüsslein-Volhard, C. (1988). A group of genes required for pattern formation in the ventral ectoderm of the Drosophila embryo. *Genes Dev.* **2,** 1496–1511.

Menne, T. V., and Klämbt, C. (1994). The formation of commissures in the Drosophila CNS depends on the midline cells and on the Notch gene. *Development* **120,** 123–133.

Menne, T. V., Luer, K., Technau, G. M., and Klämbt, C. (1997). CNS midline cells in Drosophila induce the differentiation of lateral neural cells. *Development* **124,** 4949–4958.

Mitchell, K. J., Doyle, J. L., Serafini, T., Kennedy, T. E., Tessier-Lavigne, M., Goodman, C. S., and Dickson, B. J. (1996). Genetic analysis of Netrin genes in Drosophila: Netrins guide CNS commissural axons and peripheral motor axons. *Neuron* **17,** 203–215.

Monge, I., Krishnamurthy, R., Sims, D., Hirth, F., Spengler, M., Kammermeier, L., Reichert, H., and Mitchell, P. J. (2001). Drosophila transcription factor AP-2 in proboscis, leg and brain central complex development. *Development* **128,** 1239–1252.

Morel, V., and Schweisguth, F. (2000). Repression by suppressor of hairless and activation by Notch are required to define a single row of single-minded expressing cells in the Drosophila embryo. *Genes Dev.* **14,** 377–388.

Muralidhar, M. G., Callahan, C. A., and Thomas, J. B. (1993). Single minded regulation of genes in the embryonic midline of the Drosophila central nervous system. *Mech. Dev.* **41,** 129–138.

Nambu, J. R., Franks, R. G., Hu, S., and Crews, S. T. (1990). The single minded gene of Drosophila is required for the expression of genes important for the development of CNS midline cells. *Cell* **63,** 63–75.

Nambu, J. R., Lewis, J. O., Wharton, K. A., Jr., and Crews, S. T. (1991). The Drosophila single minded gene encodes a helix loop helix protein that acts as a master regulator of CNS midline development. *Cell* **67,** 1157–1167.

Ohshiro, T., and Saigo, K. (1997). Transcriptional regulation of breathless FGF receptor gene by binding of TRACHEALESS/dARNT heterodimers to three central midline elements in Drosophila developing trachea. *Development* **124,** 3975–3986.

Patel, N. H., Snow, P., and Goodman, C. S. (1987). Characterization and cloning of fasciclin III: A glycoprotein expressed on a subset of neurons and axon pathways in *Drosophila*. *Cell* **48,** 975–988.

Poulson, D. F. (1950). Histogenesis, organogenesis, differentiation in the embryo of *Drosophila melanogaster*. In "Biology of Drosophila" (M. Demerec, Ed.), pp. 168–274. Wiley, New York.

Rothberg, J. M., Hartley, D. A., Walther, Z., and Artavanis-Tsakonas, S. (1988). *slit*: An EGF-homologous locus in *Drosophila melanogaster* involved in the development of the embryonic central nervous system. *Cell* **55,** 1047–1059.

Rothberg, J. M., Jacobs, J. R., Goodman, C. S., and Artavanis-Tsakonas, S. (1990). slit: An extracellular protein necessary for development of midline glia and commissural axon pathways contains both EGF and LRR domains. *Genes Dev.* **4,** 2169–2187.

Sanchez, L., and Guerrero, I. (2001). The development of the Drosophila genital disc. *Bioessays* **23,** 698–707.

Schuster, S., and Götz, K. G. (1994). Adaptation of area covering random walk in Drosophila. In "In Sensory Transduction" (N. Elsner and H. Breer, Eds.), Vol. II, pp. 304. Thieme, Göttingen.

Selleck, S. B., and Steller, H. (1991). The influence of retinal innervation on neurogenesis in the first optic ganglion of Drosophila. *Neuron* **6,** 83–99.

Simon, A. F., Boquet, I., Synguelakis, M., and Preat, T. (1998). The Drosophila putative kinase linotte (derailed) prevents central brain axons from converging on a newly described interhemispheric ring. *Mech. Dev.* **76,** 45–55.

Sonnenfeld, M., Ward, M., Nystrom, G., Mosher, J., Stahl, S., and Crews, S. (1997). The Drosophila tango gene encodes a bHLH PAS protein that is orthologous to mammalian Arnt and controls CNS midline and tracheal development. *Development* **124,** 4571–4582.

Sonnenfeld, M. J., and Jacobs, J. R. (1994). Mesectodermal cell fate analysis in Drosophila midline mutants. *Mech. Dev.* **46,** 3–13.

Soriano, N. S., and Russell, S. (1998). The Drosophila SOX domain protein Dichaete is required for the development of the central nervous system midline. *Development* **125,** 3989–3996.

Stollewerk, A., Klämbt, C., and Cantera, R. (1996). Electron microscopic analysis of Drosophila midline glia during embryogenesis and larval development using beta galactosidase expression as endogenous cell marker. *Microsc. Res. Tech.* **35,** 294–306.

Strauss, R. (1998). Automatische Diagnose genetisch bedingter Laufanomalien der Fliege Drosophila bei freier Bewegung in realer und virtueller Umgebung. In "In Forschung und wissenschaftliches Rechnen. GWDG-Bericht Nr. 51, " (T. Plesser and P. Wittenburg, Eds.), pp. 53–78. Gesellschaft für wissenschaftliche Datenverarbeitung mbH Göttingen, Göttingen.

Strauss, R., and Heisenberg, M. (1993). A higher control center of locomotor behavior in the Drosophila brain. *J. Neurosci.* **13,** 1852–1861.

Strauss, R., and Pichler, J. (1998). Persistence of orientation toward a temporarily invisible landmark in Drosophila melanogaster. *J. Comp. Physiol.* [*A*] **182,** 411–423.

Strauss, R., Schuster, S., and Gotz, K. G. (1997). Processing of artificial visual feedback in the walking fruit fly *Drosophila melanogaster*. *J. Exp. Biol.* **200,** 1281–1296.

Strauss, R., and Trinath, T. (1996). Is walking in a straight line controlled by the central complex? Evidence from a new Drosophila mutant. In "Göttingen Neurobiology Report" (N. Elsner and H.-U. Schnitzler, Eds.), Vol. II. Thieme, Göttingen.

Therianos, S., Leuzinger, S., Hirth, F., Goodman, C. S., and Reichert, H. (1995). Embryonic development of the Drosophila brain: Formation of commissural and descending pathways. *Development* **121,** 3849–3860.

Thomas, J. B., Crews, S. T., and Goodman, C. S. (1988). Molecular genetics of the single-minded locus: A gene involved in the development of the Drosophila nervous system. *Cell* **52,** 133–141.

Ward, M. P., Mosher, J. T., and Crews, S. T. (1998). Regulation of bHLH PAS protein subcellular localization during Drosophila embryogenesis. *Development* **125,** 1599–1608.

Zhou, L., Xiao, H., and Nambu, J. R. (1997). CNS midline to mesoderm signaling in Drosophila. *Mech. Dev.* **67,** 59–68.

Received for publication May 14, 2002
Revised June 27, 2002
Accepted June 27, 2002
Published online August 19, 2002